

## UvA-DARE (Digital Academic Repository)

### Spectroscopy and dynamics of excited states in maleimide and N-methyl maleimide: ionic projection and ab initio calculations

ter Steege, D.H.A.; Buma, W.J.

DOI

[10.1063/1.1574803](https://doi.org/10.1063/1.1574803)

Publication date

2003

Published in

Journal of Chemical Physics

[Link to publication](#)

#### Citation for published version (APA):

ter Steege, D. H. A., & Buma, W. J. (2003). Spectroscopy and dynamics of excited states in maleimide and N-methyl maleimide: ionic projection and ab initio calculations. *Journal of Chemical Physics*, 118, 10944-10955. <https://doi.org/10.1063/1.1574803>

#### General rights

It is not permitted to download or to forward/distribute the text or part of it without the consent of the author(s) and/or copyright holder(s), other than for strictly personal, individual use, unless the work is under an open content license (like Creative Commons).

#### Disclaimer/Complaints regulations

If you believe that digital publication of certain material infringes any of your rights or (privacy) interests, please let the Library know, stating your reasons. In case of a legitimate complaint, the Library will make the material inaccessible and/or remove it from the website. Please Ask the Library: <https://uba.uva.nl/en/contact>, or a letter to: Library of the University of Amsterdam, Secretariat, Singel 425, 1012 WP Amsterdam, The Netherlands. You will be contacted as soon as possible.

# Spectroscopy and dynamics of excited states in maleimide and N-methyl maleimide: Ionic projection and *ab initio* calculations

D. H. A. ter Steege and W. J. Buma<sup>a)</sup>

Faculty of Science, Institute of Molecular Chemistry, University of Amsterdam,  
Nieuwe Achtergracht 127–129, 1018 WS Amsterdam, The Netherlands

(Received 13 February 2003; accepted 25 March 2003)

The state that is responsible for the strong one-photon absorption around 200 nm in the vapor absorption spectrum of maleimide and N-methyl maleimide has been investigated using excited-state photoelectron spectroscopy in combination with *ab initio* calculations. The projection of the wave function of the excited state on the ionic manifold done in this way reveals multiple, vibrationally resolved, ionization pathways to ground- and excited states of the radical cation, which provide direct evidence for electronic couplings with other, lower-lying states. From a comparison of the experimental intensity distribution over the ionic vibrational states with *ab initio* calculated Franck–Condon factors, we are able to elucidate the role of the various electronically excited states in the ionization process. The experiments also provide the first determination of adiabatic ionization energies in the two molecules. For maleimide values of 10.330 and 10.903 eV are found for  $D_0$  and  $D_1$ , respectively; for N-methyl maleimide  $D_0$  is found at 9.897 eV or, in an alternative interpretation of the spectrum, at 9.676 eV. Calculations and experiment demonstrate that in this molecule the ground ionic state changes its character with respect to maleimide from a lone pair to a  $\pi$  orbital ionization. © 2003 American Institute of Physics. [DOI: 10.1063/1.1574803]

## I. INTRODUCTION

Excited-state photoelectron spectroscopy has in recent years emerged as a powerful means to obtain a detailed characterization of an excited state. Basically, what one does is to project the electronic and vibrational wave function of the excited state onto the rovibronic manifold of the radical cation. Most often this is done employing the ground-state  $D_0$  of the radical cation to provide the basis functions for the projection,<sup>1,2</sup> but other radical cationic states can be used to one's advantage as well (Refs. 3–5, and references therein). Electronic relaxation dynamics is an example of a research area where the projection on one or more electronic ionic states has proven to be particularly rewarding. Time-resolved photoelectron spectroscopy can in these cases provide an excellent view of the internal conversion pathways and the nonadiabatic vibronic couplings that lie at their origin. A recent study of Stolow *et al.* gives in this respect a good overview of what has been done up till now.<sup>5</sup> A useful concept that was introduced in the studies of Stolow *et al.* was that of corresponding<sup>4</sup> and complementary<sup>3</sup> ionization correlations, i.e., the ionization behavior of coupled states that correlate with the same and with different ionic states, respectively.

In most of the time-resolved studies, the *vibrational* resolution in the photoelectron spectrum was of secondary importance; what counted primarily was that one was able to make a distinction between either different ionic states that were accessed in the case of complementary ionization, or differences in the total ionic vibrational content in the case of

corresponding ionization. We have demonstrated that the complementary approach of concentrating on the energy resolution in the frequency domain—as opposed to time resolution in the time domain—enables one to disentangle vibronically coupled states as well.<sup>1,2,6</sup> As might be expected, these studies show that the frequency domain approach has its own distinct advantages, in particular for close-lying states that ionize to the same electronic ionic state. Application to complementary ionization channels has, however, not been done so far, but is one of the subjects of interest in the present study on maleimide and N-methyl maleimide.

Photoinduced polymer synthesis is a continuously growing field in which maleimide and its N-substituted derivatives (Fig. 1) have attracted considerable interest. It has been known for quite some time now that N-substituted maleimides easily polymerize by a free-radical polymerization process upon exposure to light.<sup>7</sup> N-substituted maleimides can thus serve as photoinitiators for the free-radical polymerization and copolymerization of a variety of functional species including acrylate, vinyl ether, and styryloxy monomers.<sup>8–17</sup> To give one particular example, in the aerospace industry bismaleimides are widely used because of the advantage they offer density wise, while maintaining mechanical properties that are similar to metal alloys. The first step in initiating the free-radical polymerization reaction with these compounds is excitation of the maleimide chromophore. Intersystem crossing, of which the quantum yield has been shown to be very sensitive to substitution,<sup>18</sup> leads then to population of the lowest excited triplet state. This triplet species reacts with hydrogen atom donors such as alcohols and ethers via direct hydrogen atom abstraction, or with amines and vinyl ethers via an electron-transfer/proton-transfer reaction sequence ini-

<sup>a)</sup> Author to whom correspondence should be addressed. Electronic mail: wybren@science.uva.nl

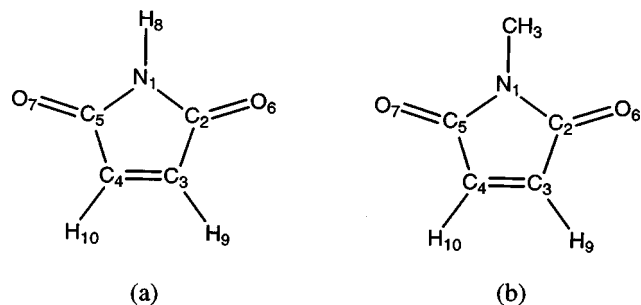


FIG. 1. Molecular structure of (a) maleimide and (b) N-methyl maleimide, as well as employed labeling of atoms.

tiating the free-radical polymerization reaction.<sup>19,20</sup> Maleimide has also been employed in a variety of photochemical applications. One such application is based on the electron accepting properties of maleimide. It has been shown that these properties can form the basis for modulating the fluorescence of compounds in which maleimide is incorporated. This modulation, in turn, can be used to probe polymerization dynamics<sup>21</sup> or as a molecular sensor.<sup>22</sup>

Applications such as the ones mentioned above revolve around the interaction of the molecule with light and involve electronically excited states, and one might therefore assume that the electronic spectroscopy and dynamic properties of the excited states of the molecule and its derivatives would have been studied extensively. The opposite is true. One of the first studies specifically dedicated to the electronic properties of the molecule was done by Matsuo,<sup>23</sup> who claimed that in n-hexane the absorption band of lowest energy was located at about 270 nm, and should be assigned to a  $\pi\pi^*$  transition. These results were later revised in a series of studies by Seliskar and McGlynn,<sup>24–26</sup> who found four electronic valence transitions below 6.5 eV. The lowest absorption band of maleimide in apolar solvents was found at 372 nm ( $\sim 26\,880\text{ cm}^{-1}$ ) and assigned as the transition to an  $n\pi^*$  state. At higher excitation energies, two more bands were found around 280 and 200 nm that were assigned as  $\pi\pi^*$  transitions. Finally, a weak emission starting at 443 nm was found that was attributed to the  $T_1 \leftarrow S_0$  transition. From its lifetime, it was concluded that this  $T_1$  state is an  $n\pi^*$  state. The N-methyl-substituted compound has also been investigated in these studies. For this molecule two  $^1\pi\pi^*$  transitions were reported, the lower-energy one exhibiting a marked redshift ( $\sim 3800\text{ cm}^{-1}$ ) with respect to its parent compounds, the second one being less sensitive to methyl substitution ( $\sim 500\text{ cm}^{-1}$ ).

The present study has a twofold aim. On the one hand, we wish to elucidate the spectroscopic properties of the strongest one-photon absorbing state located around 200 nm in maleimide and N-methyl maleimide. To this purpose we have employed (1 + 1) resonance enhanced multiphoton ionization (REMPI) spectroscopy. Absorption in the 200 nm band populates a higher excited state that is subject to internal conversion processes. The second aim of our studies is to study the underlying vibro–electronic couplings between the various states in the frequency domain by vibrationally resolved excited-state photoelectron spectroscopy. That the

maleimide system is particularly adapted for such studies can be anticipated from the results of semiempirical calculations by Seliskar and McGlynn.<sup>26</sup> There it was seen that a limited number of molecular orbitals are important for the description of the lower excited states of the neutral molecule. Preliminary *ab initio* calculations performed by us confirmed this picture: for maleimide of  $C_{2v}$  symmetry it was found that the relevant orbitals are the symmetric  $n_o^+(a_1)$  and antisymmetric  $n_o^-(b_2)$  combinations of the lone pair orbitals on the oxygen atoms, a C=C bonding  $\pi$  orbital ( $b_1$ ) that we will label as  $\pi_{C=C}$ , a  $\pi$  orbital ( $b_1$ ) that has a dominant contribution from the nitrogen atom and is labeled as  $\pi_N$ , and an antibonding  $\pi^*$  orbital ( $a_2$ ). The lower excited singlet states are then in first approximation described by the ( $\pi^* \leftarrow n_o^-$ ) excitation ( $S_1$ ), the ( $\pi^* \leftarrow n_o^+$ ) excitation ( $S_2$ ), while the  $\pi\pi^*$  states  $S_3$  and  $S_4$  are described by combinations of the ( $\pi^* \leftarrow \pi_{C=C}$ ) and ( $\pi^* \leftarrow \pi_N$ ) excitations. Although we do not yet know anything on the ordering and composition of the electronic states of the radical cation, it is reasonable to expect that when these configurations are ionized, each of them is associated with a unique ionic state:  $S_1$  correlates with the  $(n_o^-)^{-1}$  state,  $S_2$  with the  $(n_o^+)^{-1}$  state, while  $S_3$  and  $S_4$  correlate with states based upon the  $(\pi_N)^{-1}$  and  $(\pi_{C=C})^{-1}$  configurations.

The state associated with the strong 200 nm absorption is the  $S_4(\pi\pi^*)$  state. The above considerations lead to the conclusion that, if this state is coupled to any of the lower-lying states, one might distinguish the contributions to the (coupled) wave function by selection of the appropriate ionization channel. Coupling to  $S_1$ —or, in the time domain, internal conversion to this state—for example, should become visible by population of the  $(n_o^-)^{-1}$  ionic state, which is not accessible from  $S_4$ . On the basis of their electronic description, we can anticipate that the equilibrium geometry and force fields of the states of interest ( $S_1$  to  $S_4$ ) are different. This implies that if ionization of the contributing states in the coupled wave function would take place to the same ionic state, one might still distinguish the various contributions by their gross vibrational content, but in particular by the Franck–Condon pattern in a vibrationally resolved photoelectron spectrum. The experimental results that are obtained by excited-state photoelectron spectroscopy will therefore be combined with extensive *ab initio* calculations. It will be shown that we can characterize in this way in quite some detail the spectroscopic and dynamic properties of the strongly absorbing  $\pi\pi^*$  state of maleimide and N-methyl maleimide. Apart from elucidating the electronic structure of the neutral molecules, the present study provides us with an comprehensive view on the electronic structure of the radical cation of the two species.

## II. EXPERIMENTAL AND THEORETICAL DETAILS

The experiments reported in this study have been performed using a setup that has been described in detail before.<sup>27,28</sup> Here, we will therefore only summarize some of the aspects that are relevant for the present experiments. The laser setup consists of a pulsed dye laser (Lumonics Hyperdye-300) running on Coumarine 440, which is pumped

by a XeCl excimer laser (Lambda Physik EMG103-MS). The excimer laser gives 10 ns pulses with a maximum pulse energy of 200 mJ and is predominantly used at a repetition rate of 30 Hz. The dye laser output with a spectral bandwidth of about  $0.07 \text{ cm}^{-1}$  was frequency doubled using an angle-tuned BBO crystal in an INRAD Autotracker II unit, and focused into the ionization region of the magnetic bottle spectrometer<sup>29</sup> that is interfaced with a molecular beam expansion.<sup>27</sup> So far, we have employed this spectrometer in experiments in which an excited state is predominantly populated by absorption of more than one photon, and therefore used a lens with a focal length of 25 mm. In the present experiments one-photon excitation is used, for which a 25 mm lens gave rise too easily to saturation effects. The 25 mm lens was therefore replaced by a 225 mm lens. Theoretically, this might give rise to a worse resolution in the photoelectron spectra (*vide infra*)<sup>29</sup> because of the large focal volume, but in practice we could still obtain the same—or slightly worse—resolution as became clear from calibration experiments on xenon.

In order to have enough vapor pressure of the compound under investigation, the sample is put into a sample container that can be heated. When the sample needs to be heated, the temperature of the 0.5 mm nozzle (General Valve Iota One System) is normally kept  $10^\circ\text{C}$  higher than the sample container in order to avoid condensation in the injector. N-methyl maleimide has a vapor pressure at room temperature of  $>200 \text{ mTorr}$ , and, when heated up to  $90^\circ\text{C}$ , was not difficult to study under supersonic beam conditions. Maleimide, on the other hand, has a negligible vapor pressure at room temperature. Upon heating we could observe some signal under supersonic beam conditions, but not enough to record excited-state photoelectron spectra of good enough quality. We have therefore also performed experiments on effusively introduced samples. In those experiments the sample did not need to be heated, because enough vapor pressure was generated by simply pumping on the sample. Maleimide and N-methyl maleimide were obtained from Aldrich and employed as supplied.

Excitation spectra have been constructed by integration of (part of) the photoelectrons over the scanned wavelength region. Photoelectron spectra have been recorded by increasing in steps the retarding voltage on a grid surrounding the flight tube, and transforming each time only the high-resolution part of the time-of-flight spectrum. For wavelengths above  $\sim 240 \text{ nm}$  the photoelectron peaks have widths of about 10 meV at all kinetic energies. For shorter wavelengths, the resolution becomes progressively worse to such an extent that near 225 nm—the wavelength region employed in the present experiments—the width of the photoelectron peaks increases to about 25 meV. The energy scale of the photoelectrons as well as the laser wavelengths were calibrated using multiphoton resonances of krypton or xenon.<sup>30</sup>

Density functional theory (DFT) and time-dependent DFT (TD-DFT) calculations on the ground- and excited states of maleimide and N-methyl maleimide in its neutral and radical cationic form have been performed employing the GAUSSIAN 98 suite of programs.<sup>31</sup> For the complete active

TABLE I. Geometrical parameters ( $\text{\AA}$  and degrees) of maleimide in its neutral and ionic ground state.

	$S_0$	$S_0$	$D_0$
	Experiment <sup>a</sup>	B3LYP/6-311+G*	UB3LYP/6-311+G*
H–C	1.096 <sup>b</sup>	1.081	1.082
H–N	1.025 <sup>b</sup>	1.009	1.017
C=C	1.344	1.334	1.323
C–C	1.508	1.503	1.517
C–N	1.409	1.396	1.394
C=O	1.206	1.206	1.199
C–N–C	112.0	111.8	109.4
N–C–C	106.8	105.1	107.0
N–C=O	123.9	126.4	123.1
C <sub>5</sub> –C <sub>4</sub> –H <sub>10</sub> <sup>c</sup>		121.7	120.8

<sup>a</sup>From Ref. 39.

<sup>b</sup>Assumed parameters in Ref. 39.

<sup>c</sup>Reference 39 reports a C–C–H angle of  $114.7^\circ$ , but it is not clear from the paper which angle is reported. Reference 48 reports an electron diffraction study in which an average value of  $125.5^\circ$  is obtained for the C<sub>9</sub>–C<sub>10</sub>–H<sub>8</sub> angle, but in the crystal the geometry of the molecule is affected by intermolecular hydrogen bonds and dimeric interactions.

space self-consistent-field (CASSCF) calculations on the excited states of maleimide, the GAMESS-DAKOTA package has been used.<sup>32</sup> Franck–Condon factors have been evaluated with an in-house-written program<sup>33</sup> that is based upon the methods developed by Doktorov *et al.*<sup>34</sup>

### III. RESULTS AND DISCUSSION

In the following we will present and discuss the excitation and photoelectron spectra that have been obtained for maleimide and N-methyl maleimide in the energy region where the strong absorption to the  $2^1B_1$  ( $\pi\pi^*$ ) state is located. As we have demonstrated amply before,<sup>1,2,6,35</sup> an optimal analysis of photoelectron spectra requires knowledge of the vibrational frequencies in the ionic state to which ionization occurs. As yet, however, virtually nothing is known about these frequencies, but our experience is that—at least for the ground state of the radical cation—an accurate enough prediction can be obtained from density functional theory calculations. During the analysis of our results, it also became clear that not only an accurate description of the ground electronic state of the radical cation was needed, but of the excited states of the neutral molecule and of the radical cation as well. Prior to discussing the experimental results, we will therefore in the next sections present the results of our *ab initio* calculations, and subsequently use them to guide the interpretation of our experimental results.

#### A. Maleimide

##### 1. *Ab initio* calculations

Optimization of the molecular geometry of maleimide in its electronic ground state  $S_0$  at the B3LYP/6-311+G\*<sup>36–38</sup> level leads to a  $C_{2v}$  structure with structural parameters reported in Table I. Good agreement is observed with parameters as determined in an electron diffraction study of maleimide in the gas phase.<sup>39</sup> The electronic configuration at this geometry is given by  $\cdots(2b_1)^2(12a_1)^2(3b_1)^2(9b_2)^2$ . From the orbital contour plots shown in Fig. 2, it is seen that the relevant  $\pi$  orbitals of  $b_1$  symmetry can roughly be char-



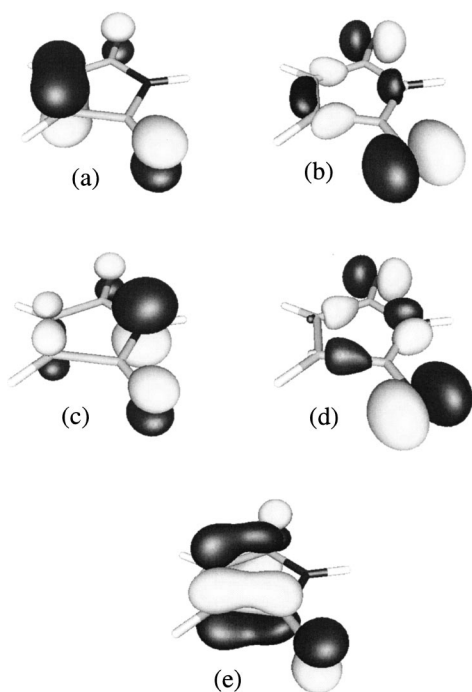


FIG. 2. Contour plots of the (a)  $2b_1$  ( $\pi_{C=C}$ ), (b)  $12a_1$  ( $n_o^+$ ), (c)  $3b_1$  ( $\pi_N$ ), (d)  $9b_2$  ( $n_o^-$ ), and (e)  $2a_2$  ( $\pi_{C-C}^*$ ) molecular orbitals of maleimide.

acterized as being localized on the nitrogen atom ( $2b_1 = \pi_{C=C}$ ) and the C=C bond ( $3b_1 = \pi_N$ ). The in-plane  $12a_1$  and  $9b_2$  orbitals consist of the symmetric and antisymmetric combination of the oxygen lone pair orbitals, respectively,

and will be designated as  $n_o^+$  and  $n_o^-$ . In the following, we will see that the lower-lying excited states of interest in the present studies are in first approximation described as excitations of electrons from these  $\pi$ - and  $n$  orbitals to the  $2a_2(\pi^*)$  orbital. The contours of this virtual orbital, which will be designated as  $\pi_{C-C}^*$ , are depicted in Fig. 2, and show that it is characterized by bonding C-C and antibonding C=C character.

The ground state  $D_0$  of the radical cation derives in our calculations from the removal of an electron from the  $9b_2(n_o^-)$  orbital, resulting in a state of  ${}^2B_2$  symmetry. Optimization of the geometry of the molecule in this state results in a structure with  $C_{2v}$  symmetry and structural parameters that are given in Table I. In line with the nonbonding character of the  $n_o^-$  orbital, the geometry of the molecule is hardly affected by the removal of an electron from this orbital.

The vibrational frequencies obtained from the calculation of the harmonic force field for both states are listed in Table II. For the ground state of the neutral molecule excellent agreement is found between (scaled) calculated values and experimental frequencies determined by infrared and Raman spectroscopy.<sup>40-42</sup> For the ground state of the radical cation, vibrational frequencies have not yet been determined experimentally.

To investigate the excited-state manifold of the neutral and radical cation, we have used time-dependent density functional theory calculations at their (U)B3LYP/6-311 + G\* optimized geometries, once again with the B3LYP

TABLE II. Experimental and *ab initio* vibrational frequencies ( $\text{cm}^{-1}$ ) of ground and ionic states of maleimide.

Symmetry	Mode	$S_0^a$ B3LYP	$S_0^b$ Experiment	$D_0^a$ UB3LYP	Description <sup>c</sup>
$a_1$	$\nu_1$	3536	3482	3447	$\nu\text{N-H}$
	$\nu_2$	3145	3090	3147	$\nu\text{C-H}$
	$\nu_3$	1793	1775	1719	$\nu\text{C=O}$
	$\nu_4$	1592	1580	1584	$\nu\text{C=C}$
	$\nu_5$	1295	1335	1173	$\nu\text{C-N-C}$
	$\nu_6$	1045	1067 <sup>d</sup>	1044	$\delta\text{C-H}$
	$\nu_7$	874	897	822	$\nu\text{C-C}$
	$\nu_8$	621	637	609	Ring deformation
	$\nu_9$	380	415 <sup>d</sup>	360	$\delta\text{C=O}$
$a_2$	$\nu_{10}$	940	972 <sup>d</sup>	851	$\gamma\text{C-H}$
	$\nu_{11}$	758	776 <sup>d</sup>	581	Ring deformation
	$\nu_{12}$	287	301 <sup>d</sup>	276	$\gamma\text{C=O}$
$b_1$	$\nu_{13}$	821	831	792	$\gamma\text{C-H}$
	$\nu_{14}$	616	721 <sup>d</sup>	596	$\nu\text{N-H}$
	$\nu_{15}$	522	635 <sup>d</sup>	517	Ring deformation
	$\nu_{16}$	135	175 <sup>d</sup>	149	$\gamma\text{C=O}$
$b_2$	$\nu_{17}$	3124	3108 <sup>d</sup>	3129	$\nu\text{C-H}$
	$\nu_{18}$	1758	1756	1508	$\nu\text{C=O}$
	$\nu_{19}$	1318	1322	1313	$\delta\text{N-H}$
	$\nu_{20}$	1277	1285	1220	$\delta\text{C-H}$
	$\nu_{21}$	1092	1130	907	$\nu\text{C-N-C}$
	$\nu_{22}$	888	906	649	Ring deformation
	$\nu_{23}$	651	668	611	Ring deformation
	$\nu_{24}$	520	504	475	$\delta\text{C=O}$

<sup>a</sup>After scaling with factor 0.9676 (Ref. 49).

<sup>b</sup>Vapor phase values taken from Ref. 40, except those labeled d.

<sup>c</sup>Description appropriate for  $S_0$ ;  $\nu$ =stretch;  $\delta$ =in-plane bend;  $\gamma$ =out-of-plane bend.

<sup>d</sup>Raman values taken from Ref. 40.

TABLE III. Description of the ground- and lower-lying electronic excited states of neutral maleimide and of the ground and first excited states of its radical cation. For the singlet states of the neutral molecule, vertical excitation energies and oscillator strengths have been calculated by TD-DFT at the B3LYP/6-311+G\* optimized  $S_0$  ( $1^1A_1$ ) geometry; for the radical cation excitation energies have been calculated by TD-DFT at the UB3LYP/6-311+G\* optimized geometry of the  $D_0$  ( $X^2B_2$ ) state of the radical cation. The adiabatic excitation energy of the  $T_1$  ( $1^3B_1$ ) state was calculated at the UB3LYP/6-311+G\* level.

State	Description	Energy (eV)	Oscillator strength
$S_0$ ( $1^1A_1$ )	$(\pi_{C=C})^2(n_o^+)^2(\pi_N)^2(n_o^-)^2$	0	
$S_1$ ( $1^1B_1$ )	$(\pi_{C=C})^2(n_o^+)^2(\pi_N)^2(n_o^-)^1(\pi_{C-C}^*)^1$	3.46	0.0000
$S_2$ ( $1^1A_2$ )	$(\pi_{C=C})^2(n_o^+)^1(\pi_N)^2(n_o^-)^2(\pi_{C-C}^*)^1$	4.23	0.0000
$S_3$ ( $1^1B_2$ )	$(\pi_{C=C})^2(n_o^+)^2(\pi_N)^1(n_o^-)^2(\pi_{C-C}^*)^1$	4.51	0.0046
$S_4$ ( $2^1B_2$ )	$(\pi_{C=C})^1(n_o^+)^2(\pi_N)^2(n_o^-)^2(\pi_{C-C}^*)^1$	5.77	0.3222
$T_1$ ( $1^3B_1$ )	$(\pi_{C=C})^2(n_o^+)^2(\pi_N)^2(n_o^-)^1(\pi_{C-C}^*)^1$	2.84	
$D_0$ ( $X^2B_2$ )	$(\pi_{C=C})^2(n_o^+)^2(\pi_N)^2(n_o^-)^1$	0	
$D_1$ ( $A^2B_1$ )	$-0.69 (\pi_{C=C})^2(\pi_{C=C})^1(n_o^+)^2(\pi_N)^2(n_o^-)^2$ $+0.82 (\pi_{C=C})^2(\pi_{C=C})^2(n_o^+)^2(\pi_N)^1(n_o^-)^2$	0.63	
$D_2$ ( $B^2B_1$ )	$0.85 (\pi_{C=C})^2(\pi_{C=C})^1(n_o^+)^2(\pi_N)^2(n_o^-)^2$ $+0.62 (\pi_{C=C})^2(\pi_{C=C})^2(n_o^+)^2(\pi_N)^1(n_o^-)^2$	0.93	

functional. For the four lower excited states of the neutral molecule electron configurations, excitation energies and oscillator strengths are reported in Table III. We find that the first excited singlet state ( $1^1B_1$ ) is an  $n\pi^*$  state obtained by excitation of an electron from the  $n_o^-$  to the  $\pi_{C-C}^*$  orbital. The essentially forbidden  $1^1B_1 \leftarrow 1^1A_1$  transition has a calculated transition energy of 3.46 eV (27 900  $\text{cm}^{-1}$ ), which agrees very well with the study of Seliskar and McGlynn, in which a very weak  $n\pi^*$  transition at  $\sim 360$  nm (3.3 eV) was reported.<sup>24</sup> The second excited singlet state,  $1^1A_2$ , is a one-photon symmetry-forbidden  $n\pi^*$  transition described by excitation of an electron from the  $n_o^+$  orbital to the  $\pi_{C-C}^*$  orbital. The third and fourth excited singlet states are of  $\pi\pi^*$  character, with  $S_3$  ( $1^1B_2$ ) being dominated by the  $\pi_N \rightarrow \pi_{C-C}^*$  configuration and  $S_4$  ( $2^1B_2$ ) by the  $\pi_{C=C} \rightarrow \pi_{C-C}^*$  configuration. Experimentally, two  $\pi\pi^*$  transitions have been observed with vertical excitation energies of 4.4 and 5.9 eV, respectively. These excitation energies compare well with the values of 4.51 and 5.77 eV obtained in our calculations. For the  $S_4 \leftarrow S_0$  transition, experimental and predicted values of the oscillator strength are in excellent agreement (0.31 vs 0.32). The calculations predict a small oscillator strength for the transition to  $S_3$ , while experimentally a value of 0.24 was reported. This latter value seems rather high considering that molar extinction coefficients of 750 and 10 000  $\text{M}^{-1}\text{cm}^{-1}$  were found for the  $S_3$  and  $S_4$  transitions, respectively. The reason for the discrepancy between the experimental and calculated values of the oscillator strength of the transition to  $S_3$  is not clear, but for the present discussion not directly important. One other state of interest to the present study that has been investigated in the past is the lowest excited triplet state  $T_1$ . TD-DFT as well as UB3LYP calculations find this state to be the  $1^3B_1$  ( $n_o^+\pi_{C-C}^*$ ) state with an adiabatic excitation energy of 2.84 eV ( $\sim 23$  000  $\text{cm}^{-1}$ ), which is in excellent agreement with the experimentally observed value.

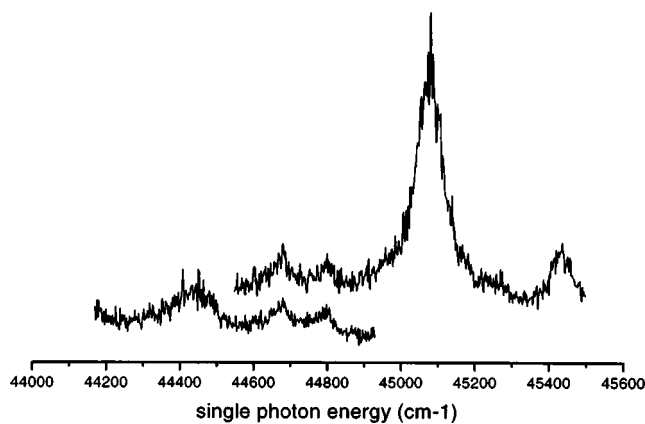


FIG. 3. (1+1) REMPI excitation spectrum of effusively introduced maleimide. The spectrum consists of two scans that have been displayed vertically for reasons of clarity.

For the radical cation we are in the present study mainly interested in the ground- and first excited state. The ground state  $D_0$  ( $X^2B_2$ ) is described by removal of an electron from the  $n_o^-$  orbital. Our calculations predict, for the vertical and adiabatic ionization energies to  $D_0$ , values of 10.286 and 10.219 eV, respectively. The relatively small difference of 67 meV is in agreement with our conclusion above on the (non-bonding) character of the  $n_o^-$  orbital. Experimental values for the ionization energy of maleimide have thus far not been reported, but the calculated value is not in disagreement with the value of 9.991 eV that has been reported for the vertical ionization energy of N-methylmaleimide<sup>43</sup> (see also below, however). The first excited state in the ionic manifold is the  $A^2B_1$  state, predicted to lie 0.63 eV above the  $X^2B_2$  state. This state is largely about an 1:1 mixture of configurations with a hole in the  $\pi_{C=C}$  or in the  $\pi_N$  orbital. Its counterpart is the second excited  $B^2B_1$  state, which is located 0.93 eV above the ionic ground state.

## 2. Multiphoton ionization and excited-state photoelectron spectroscopy

A (1+1) REMPI excitation spectrum of maleimide, introduced effusively in the spectrometer, was recorded in the 44 000–45 500  $\text{cm}^{-1}$  spectral region, and is shown in Fig. 3. On the basis of previous absorption measurements and our *ab initio* calculations, we expect to see here the transition to the  $2^1B_2$  ( $\pi\pi^*$ ) state, and consequently assign the resonance at 45 070  $\text{cm}^{-1}$  as the vibrationless transition to this state. Compared with the same transition in N-methyl maleimide<sup>43</sup> (see also Sec. III B 2), this implies a blueshift of 480  $\text{cm}^{-1}$ , which is what may be expected for the effect of methylation. Apart from the origin transition, four more transitions are observed. The bands observed at 635 and 395  $\text{cm}^{-1}$  to the red of the  $0_0^0$  transition are readily assigned to the  $8_1^0$  and  $9_1^0$  hot band transitions on the basis of the frequencies reported in Table I. The same table shows that the band shifted by 280  $\text{cm}^{-1}$  to the red cannot be assigned to an  $a_1$  vibration. Although this frequency is similar to that of  $\nu_{12}$  in the ground state, it is hard to imagine that it would be the  $12_1^0$  hot band, because that would imply loss of symmetry in the excited state, and lead us to expect that the  $12_0^1$  transition

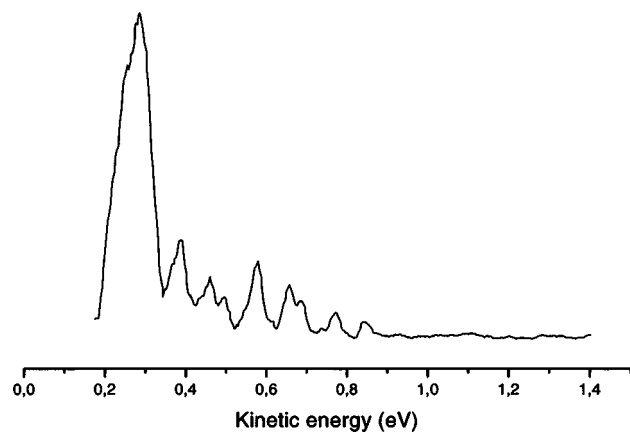


FIG. 4. Excited-state photoelectron spectrum of the vibrationless  $S_4$  excited state of maleimide excited at  $45\,070\text{ cm}^{-1}$ .

would also be observable. It is more probable that this band is associated with a  $(\nu_i)_1^+$  transition, implying that one of the modes undergoes a rather dramatic frequency decrease upon excitation, but which mode cannot be determined. The resonance at  $45\,435\text{ cm}^{-1}$  is assigned as the  $9_0^+$  transition. The observed frequency decrease in the excited state is in line with an increased antibonding character of the C=O bond upon excitation (see Fig. 2).

The photoelectron spectrum recorded at the 0–0 transition to the  $S_4$  state is depicted in Fig. 4. Before assigning the various peaks in this spectrum, it is instructive to think of what we may expect to see on the basis of the electronic composition of the excited state. Our *ab initio* calculations have shown that the dominant configuration in the wave function of  $S_4$  is the  $\pi_{\text{C}=\text{C}} \rightarrow \pi_{\text{C}=\text{C}}^*$  configuration. From these calculations we have also seen that  $D_0$  is described as the  $(n_o^-)^{-1}$  state. Within this simple one-configuration picture, ionization of  $S_4$  to  $D_0$  is thus in first approximation forbidden. Ionization to the  $D_1$  and  $D_2$ , states, which in the same picture are described by a combination of the  $(\pi_{\text{N}})^{-1}$  and  $(\pi_{\text{C}=\text{C}})^{-1}$  configurations, is on the other hand, fully allowed. The *ab initio* calculations therefore predict that the dominant ionization pathways of  $S_4$  are to  $D_1$  and  $D_2$ , and not to  $D_0$ .

The peak with the highest photoelectron energy in Fig. 4 is found at 0.846 eV. Normally, one would assume that this peak is the  $0''-0_0^+$  peak, i.e., that it derives from an ionization process that starts in the vibrationless ground state and ends up in the vibrationless  $D_0$  ionic state, but the discussion above indicates that in the present case such an assignment is not that straightforward. Nevertheless, the value of 0.846 eV leads to an ionization energy of 10.330 eV, which agrees very well with the *ab initio* predicted adiabatic value for  $D_0$  (10.22 eV), and we therefore assign this peak as the  $0''-0_0^+$  band. The strongest peak in the spectrum occurs at a photoelectron energy of 0.273 eV. Its width, which is significantly larger than the experimental resolution, indicates that it consists of various unresolved transitions. If this peak were to be associated with ionization to  $D_0$ , it would mean that ions are formed with an internal energy of 0.573 eV, and, considering its intensity relative to the  $0''-0_0^+$  band, one would have to

TABLE IV. Assignments of peaks observed in excited-state photoelectron spectrum displayed in Fig. 4 that was obtained at the 0–0 transition to  $S_4$  ( $45\,075\text{ cm}^{-1}$ ).

Electron kinetic energy (eV)	Ion internal energy ( $\text{cm}^{-1}$ )	Assignment
0.846	0	$0''-0_0^+$ ( $D_0$ )
0.772	597	$8^1$
0.739	863	$7^1$
0.688	1274	$8^2$ (or $5^1$ )
0.656	1532	$4^1$ (or $8^1 7^1$ )
0.618	1839	$8^3$ (or $3^1$ or $5^1 8^1$ )
0.575	2186	$4^1 8^1$
0.493	2847	$4^1 8^2$
0.458	3129	$4^2$
0.382	3742	$4^2 8^1$
0.273	0	$0''-0$ ( $D_1$ )

conclude that the molecule is subject to very large geometry changes upon ionization. An alternative explanation is suggested by the previous discussion on the ionization pathways of  $S_4$ , namely, that this peak derives from ionization to  $D_1$ . Our calculations predict the  $0''-0_1^+$  peak to appear with 0.63 eV less energy than the  $0''-0_0^+$  peak. The position and intensity of the 0.573 eV peak are therefore in good agreement with its assignment as the  $0''-0_1^+$  transition, and allow us to conclude that the adiabatic ionization energy to  $D_1$  is 10.903 eV. From a configurational point of view, ionization to  $D_2$  is also allowed. This pathway is not observed in the photoelectron spectrum, which is in line with the calculations that predict this state to be 0.3 eV higher in energy than  $D_1$ , and thus energetically not accessible in the present one-color experiments.

The spectrum displays a significant amount of other activity. Assuming that the molecule retains  $C_{2v}$  symmetry upon excitation, and that the ionization step can be described within the Born–Oppenheimer approximation, these bands should be associated with ionization to totally symmetric vibrational levels in the ion. As Table IV shows, we find indeed that it is not difficult to assign the spectrum in terms of ionization to vibrational levels of  $D_0$  that involve predominantly the ring deformation mode  $\nu_8^+$  and the C=C stretching vibration  $\nu_4^+$ . At the same time, it should be remarked that the resolution in the spectrum does not rule out other assignments as indicated as well for some of the entries in the same table. A possible explanation for the  $D_0$  activity is direct two-photon ionization of the ground state. This can be excluded experimentally by observing that the  $D_0$  ionization pathway is only present when resonance occurs with  $S_4$ . Theoretically, it is seen that the calculated Franck–Condon factors (*vide infra*) for the  $D_0 + e^- \leftarrow S_0$  transition, which are given in Table V, are at odds with the observed intensity distribution in the photoelectron spectrum.

In the simple model discussed above, ionization of  $S_4$  to  $D_0$  is forbidden. Nevertheless, we have now concluded that the photoelectron spectrum gives evidence for a non-negligible role of ionization to  $D_0$ . A number of explanations come to mind. The first is that the model is too simple and that  $D_0 \leftarrow S_4$  ionization is allowed in higher order. In that case, the vibrational intensity distribution in the photoelec-

TABLE V. Franck–Condon factors between the vibrationless level of various electronic states of maleimide and fundamental levels of totally symmetric vibrations in the ground ionic state  $D_0$ . The equilibrium geometry and harmonic force field of  $S_0$  and  $D_0$  have been obtained at the (U)B3LYP/6-311+G\* level, while for  $S_1$ ,  $S_2$ ,  $S_3$ ,  $S_4$ ,  $T_1$ , and  $T_4$  the CAS calculations described in the text have been employed.

Vibration	Frequency ( $\text{cm}^{-1}$ ) <sup>a</sup>	$D_0 \leftarrow$						
		$S_0$ <sup>b</sup>	$S_1$ <sup>b</sup>	$S_2$ <sup>b</sup>	$S_3$ <sup>b</sup>	$S_4$ <sup>b</sup>	$T_1$ <sup>b</sup>	$T_4$ <sup>b</sup>
$\nu_9^+$	360	40.0	6.1	7.1	2.0	0.5	4.7	13.5
$\nu_8^+$	609	35.3	29.6	55.0	359.4	71.0	26.9	51.0
$\nu_7^+$	822	8.6	146.1	153.3	143.7	129.6	138.4	144.3
$\nu_6^+$	1044	1.5	4.4	10.8	23.6	19.5	3.3	9.3
$\nu_5^+$	1173	2.7	25.4	19.8	317.9	8.4	21.3	14.6
$\nu_4^+$	1584	2.8	117.0	192.4	22.6	154.5	95.2	167.5
$\nu_3^+$	1719	0.0	75.3	148.2	39.7	32.5	62.8	130.6
$\nu_2^+$	3147	0.0	2.5	2.6	3.8	3.3	2.3	2.4
$\nu_1^+$	3447	0.2	2.6	2.8	1.4	2.0	2.6	2.8

<sup>a</sup>After scaling with factor 0.9676 (Ref. 49).

<sup>b</sup>Intensity of transition from  $0^0$  level in excited state to  $\nu_i^+(a_1)=1$  level in ionic state. Intensity is given with respect to intensity of  $0^{0+} \leftarrow 0^{0r}$  transition, which has been taken as 100.0.

tron spectrum should be proportional to the Franck–Condon factors between the vibrationless level of  $S_4$  and ionic vibrational levels, assuming of course that the  $D_0 + e^- \leftarrow S_4$  electronic transition moment is more or less independent of the vibrational coordinates. To investigate this hypothesis, we have determined the  $C_{2v}$  equilibrium geometry of the molecule in  $S_4$  at the CASSCF/6-311G\* level. The active space in these calculations consisted of the already-mentioned  $n_o^+$ ,  $n_o^-$ ,  $\pi_N$ ,  $\pi_{C=C}$ , and  $\pi_{C-C}^*$  orbitals, augmented with the  $1b_1$  and  $1a_2$   $\pi$ -, and the  $4b_1$  and  $3a_2$   $\pi^*$ -orbitals. Franck–Condon factors were then calculated from the displacement parameters with respect to the UB3LYP/6-311+G\* equilibrium geometry of the  $D_0$  state. We notice that in this approximation of the Franck–Condon factors, normal-mode rotations upon ionization are not taken into account. However, our goal at this point is to obtain qualitative agreement between experiment and theory, and because Franck–Condon factors are primarily determined by geometry changes, inclusion of normal-mode rotations is not expected to lead to major changes in the results.

The results of these calculations are shown in Table V, where the intensities for transitions from the  $0^0$  level in  $S_4$  to fundamental vibrational levels of  $a_1$  modes in  $D_0$  are given. They show that for ionization of  $S_4$  to  $D_0$  dominant activity is expected in the  $\nu_8^+$  (ring deformation),  $\nu_7^+$  (C–C stretch), and  $\nu_4^+$  (C=C stretch) modes. This agrees with the experiment insofar as  $\nu_8^+$  and  $\nu_4^+$  are concerned, but the large difference between predicted and experimental activity of  $\nu_7^+$  is distressing. Moreover, we notice that the intensity distribution in the photoelectron spectrum in Fig. 4—if attributed to ionization of a single vibrationless excited state level—can only be understood if the excited- and ionic state have very different equilibrium geometries. This is not supported by the calculated Franck–Condon factors.

The conclusion that the observed  $D_0$  activity cannot be reconciled with a mere ionization of the vibrationless level of  $S_4$  means that the  $D_0$  activity must at least in part also be associated with the ionization of another state. This implies that the “bright”  $S_4$  state, responsible for the intensity in the absorption step, is coupled to “dark” levels of another state,

which give rise to  $D_0$  activity upon ionization. At this point it is not clear to which lower-lying electronic state(s) coupling occurs, but what is interesting is that vibrational resolution is still maintained in the ionization step to  $D_0$  despite the large energy gaps with the other states (see Table III). Because of these large energy gaps, one expects to deal with nonradiative processes in the statistical limit which populate many vibrational levels, and in general lead to broad and unresolved peaks (see, for example, Refs. 44 and 45). Here we see, however, photoelectron peaks with instrument-limited widths.

The first excited singlet state  $S_1$  is a possible candidate for the state that is coupled to  $S_4$ . This state is attractive for two reasons. First,  $S_1$  is in first approximation described by the  $\pi_{C-C}^* \leftarrow n_o^-$  excitation and consequently has  $D_0 ((n_o^-)^{-1})$  as its associated ionizing state. Second, the  $S_1$  state has more than 2.5 eV of vibrational energy at the 0–0 transition energy to  $S_4$ , and the state density—and thus possibilities to couple the two states—is huge. One problem in checking this hypothesis is that we do not know which vibrational levels of  $S_1$  are coupled to the  $0^0$  level of  $S_4$ . Even so, it is reasonable to expect that the active vibrations in the photoelectron spectra of these levels are those that are associated with the differences in the equilibrium geometries of the  $S_1$  and  $D_0$  states. A measure for their activities is given by the  $I[(\nu_i^+)_0^1]/I[0_0^0]$  ratios, which have been calculated in the same way and at the same level as described above for  $S_4$ . The results given in Table V show that for  $S_1$  an ionization behavior is expected that is qualitatively similar to that of  $S_4$ . A mere ionization of high-lying vibronically coupled levels of  $S_1$  is thus also concluded to be an unlikely explanation for the observed  $D_0$  ionization pathway.

Although the first-order description of both states seems to exclude direct ionization to  $D_0$ , we have also considered the scenario that vibronic coupling occurs with high-lying vibrational levels of  $S_2$  or  $S_3$ . Optimization of the  $C_{2v}$  geometry of the molecule in these two states, and the subsequent Franck–Condon calculation leads to  $I[(\nu_i^+)_0^1]/I[0_0^0]$  intensities that are given in Table V. Apart from an enhanced  $\nu_3^+$  activity, the ionization of  $S_2$  gives rise to qualitatively the



same Franck–Condon distribution—and thus objections—that was found for  $S_4$  and  $S_1$ , i.e., strong activity of  $\nu_7^+$  and  $\nu_4^+$ , and a smaller activity of  $\nu_8^+$ . Importantly, Table V reveals that ionization of  $S_3$  is associated with a fundamentally different Franck–Condon behavior. Here, a large activity of  $\nu_8^+$  and a smaller activity of  $\nu_7^+$  is predicted, but now the activity of  $\nu_4^+$  has disappeared and has been replaced by an activity of  $\nu_5^+$  that is as large as that of  $\nu_8^+$ .

For maleimide it has been shown that the triplet quantum yield is close to unity.<sup>18</sup> Intersystem crossing might thus populate highly excited levels of a lower-lying triplet state, which are subsequently ionized into the  $D_0$  ionization continua. For experiments on a nanosecond time scale such behavior has, for example, been observed after excitation of the lowest excited singlet state of pyrazine.<sup>46</sup> The state that is excited in the present experiments is a  $\pi\pi^*$  state for which spin–orbit coupling with the lower-lying  $T_1(1^3B_1)$  and  $T_4(1^3A_2)$   $n\pi^*$  states is dominant. *A priori* one does, however, not expect that the ionization of these two states leads to Franck–Condon patterns that are much different from the ionization of their singlet counterparts, an expectation that is confirmed by and large by the calculated Franck–Condon factors in Table V. Also, ionization of triplet states is therefore not able to account for the observed intensity distribution in the photoelectron spectrum.

We thus have to conclude that the  $D_0$  activity can only be interpreted consistently if ionization occurs from more than one electronically excited state, or, in other words, from a mixed state that contains the character of various excited states. We do not claim that our calculations and experiments enable us to make a clear distinction between the contributions of the  $S_1$ ,  $S_2$ ,  $S_4$ ,  $T_1$ , and  $T_4$  states; they all give rise to a dominant activity of  $\nu_7^+$  and  $\nu_4^+$  with relatively slight variations in intensities. The latter activity is confirmed by the experiment, and leads us to conclude that one or more of these states is involved in the ionization pathway to  $D_0$ . However, at the same time our experiments show unambiguously a major activity of  $\nu_8^+$  and a minor activity of  $\nu_7^+$ , a pattern that can only be explained if ionization of  $S_3$  levels is taken into account. This conclusion implies (i) that more than one state is ionized; and (ii) that ionization of  $S_3$  should be considered beyond a simple one-configuration picture, a conclusion that also needs to be drawn in order to account for the ionization of contributing levels of  $S_4$ ,  $S_2$ , and  $T_4$ .

## B. N-methyl maleimide

### 1. *Ab initio* calculations

Calculations on N-methyl maleimide have been performed under the restriction of  $C_s$  symmetry with the mirror plane perpendicular to the ring. Optimization of the molecular geometry in  $C_s$  symmetry at the B3LYP/6-311+G\* level leads to a ground-state structure of the neutral molecule with structural parameters reported in Table VI, while the vibrational frequencies obtained from the harmonic force field at this geometry are given in Table VII. This table shows that the restriction of  $C_s$  symmetry leads to one imaginary frequency. Since it is associated with the rotation of the methyl

TABLE VI. Geometrical parameters (Å and degrees) of N-methyl maleimide in its neutral and ionic ground state.

	$S_0$	$D_0$
	B3LYP/6-311+G*	UB3LYP/6-311+G*
H–C	1.081	1.083
N–CH <sub>3</sub>	1.453	1.417
C=C	1.333	1.349
C–C	1.503	1.479
C–N	1.397	1.481
C=O	1.208	1.187
C–N–CH <sub>3</sub>	124.7	125.4
C–N–C	110.5	109.2
N–C–C	106.0	104.3
N–C=O	125.9	122.3
C <sub>5</sub> –C <sub>4</sub> –H <sub>10</sub> <sup>a</sup>	121.8	121.4

<sup>a</sup>Same angle as employed in maleimide.

group, it is not of direct importance for our discussion on the electronic properties of excited and ionic states, and we will therefore just accept it as it is.

Inspection of the contour plots of the relevant orbitals (not shown) reveals that the methyl substitution on the nitrogen atom hardly influences the electron distribution in the  $\pi_{C=C}$ ,  $n_o^+$ ,  $n_o^-$ , and  $\pi_{C-C}^*$  orbitals. The  $\pi_N$  orbital, on the other hand, obtains a significant (antibonding) density in the  $\pi$  orbital of the carbon atom of the methyl group. Concurrently, the calculations predict that the ground state of the radical cation is no longer associated with the  $(n_o^-)^{-1}$  configuration, but becomes the  $X^2A'$  state, described in first approximation by the removal of an electron from the  $\pi_N$  orbital. The UB3LYP/6-311+G\* optimized geometry of the molecule in this  $X^2A'$  state is reported in Table VI, the vibrational frequencies deriving from the harmonic force field calculation in Table VII. Since ionization to  $D_0$  now occurs from an orbital that has distinct bonding and antibonding characteristics—as opposed to maleimide, where an essentially nonbonding electron was removed—it is seen from Table VI that the geometry changes considerably upon ionization. In agreement with the antibonding density between the nitrogen atom and the methyl group in the ground state, this bond becomes shorter upon ionization. What is also important to notice is the large change in the C–N bond length, which can be interpreted as giving evidence for a large contribution of the Zwitter-ionic resonance structure in the ground state of the neutral molecule.

The results of TD–DFT calculations on the ground- and excited states of the neutral molecule are reported in Table VIII. In agreement with our qualitative conclusion that it was only the  $\pi_N$  orbital that was dominantly affected by the N-methyl substitution, we observe that the ordering and character of most of the lower-lying excited states remains the same, and that only minor changes on the order of 0.1 eV occur in the vertical excitation energy. This is not true for the  $(\pi_N \rightarrow \pi_{C-C}^*)$  state, which is redshifted by more than 0.5 eV with respect to maleimide and now becomes  $S_2$  instead of  $S_3$ . The calculated excitation energies and oscillator strengths are in good agreement with what has been observed previously in absorption spectroscopy on N-methyl maleimide in the gas phase.<sup>24</sup> That study reported two absorption

TABLE VII. Experimental and *ab initio* vibrational frequencies ( $\text{cm}^{-1}$ ) of ground and ionic states of N-methylmaleimide.

Symmetry	Mode	$S_0^a$	$S_0^b$	$D_0^a$	Description <sup>c</sup>
		B3LYP	Experiment	UB3LYP	
$a'$	$\nu_1$	3144	3103	3140	$\nu\text{C-H}$
	$\nu_2$	3022	2930	2967	$\nu\text{H-H}_3$
	$\nu_3$	2954	2903	2795	$\nu\text{C-H}_3$
	$\nu_4$	1771	1751	1817	Symmetric $\nu\text{C=O}$
	$\nu_5$	1592	1586	1534	$\nu\text{C=C}$
	$\nu_6$	1458	1456	1400	$\delta\text{C-H}_3$
	$\nu_7$	1422	1440	1315	$\delta\text{C-H}_3$
	$\nu_8$	1369	1388	1169	Symmetric $\nu\text{C-N-C}$
	$\nu_9$	1121	1150 <sup>d</sup>	1116	$r\text{C-H}_3$
	$\nu_{10}$	1103	1135	1007	$\nu\text{C-C} + \nu\text{N-CH}_3$
	$\nu_{11}$	1018	1052	975	$\delta\text{C-H}$
	$\nu_{12}$	811	832	836	$\gamma\text{C-H}$
	$\nu_{13}$	710	736	657	$\nu\text{C-C} + \nu\text{N-CH}_3$
	$\nu_{14}$	608	633	601	Ring deformation
	$\nu_{15}$	589	613	523	Ring deformation
	$\nu_{16}$	367	389	339	$\delta\text{C=O}$
	$\nu_{17}$	163	218 <sup>d</sup>	211	$\gamma\text{N-CH}_3$
	$\nu_{18}$	138	168 <sup>e</sup>	96	$\gamma\text{C=O}$
$a''$	$\nu_{19}$	3123	3080	3127	$\nu\text{C-H}$
	$\nu_{20}$	3056	2963	3045	$\nu\text{C-H}_3$
	$\nu_{21}$	1714	1701	1782	Asymmetric $\nu\text{C=O}$
	$\nu_{22}$	1478	1475	1374	$\delta\text{C-H}_3$
	$\nu_{23}$	1286	1336	1307	$\delta\text{C-H}$
	$\nu_{24}$	1238	1254	1129	Asymmetric $\nu\text{C-N-C}$
	$\nu_{25}$	1071	1108	1038	$r\text{C-H}_3$
	$\nu_{26}$	937	958	944	$\gamma\text{C-H}$
	$\nu_{27}$	924	940	782	Ring deformation
	$\nu_{28}$	752	770	618	Ring deformation
	$\nu_{29}$	684	696	578	Ring deformation
	$\nu_{30}$	553	574	551	$\delta\text{C=O}$
	$\nu_{31}$	288	299 <sup>d</sup>	244	$\gamma\text{C=O}$
	$\nu_{32}$	259	281 <sup>d</sup>	239	$\delta\text{N-CH}_3$
	$\nu_{33}$	71i	152 <sup>e</sup>	69	$\tau\text{N-CH}_3$

<sup>a</sup>After scaling with factor 0.9676 (Ref. 49).

<sup>b</sup>IR frequencies reported by Parker (Ref. 50) except those labeled d and e, which have been obtained in the same study from Raman spectroscopy and inelastic neutron scattering, respectively.

<sup>c</sup>Description appropriate for  $S_0$ ;  $\nu$ =stretch;  $\delta$ =in-plane bend;  $\gamma$ =out-of-plane bend;  $\tau$ =torsion.

bands, the lowest one being a broad band with a first observable feature at about 3.5 eV and reaching its maximum at about 4.3 eV. It was assigned as the analog of the  $S_3$  state in maleimide. The second band shows well-resolved vibrational transitions, and has its 0–0 transition at  $44\,623\text{ cm}^{-1}$  (5.53 eV).

Table VIII shows that more dramatic changes occur in the ionic manifold. Previously it was mentioned that the ground ionic state becomes the  $X^2A'((\pi_{\text{N}})^{-1})$  state for which vertical and adiabatic ionization energies of 10.074 and 9.812 eV, respectively, are calculated, their difference of 262 meV being one more reflection of the larger changes in geometry upon ionization. At the equilibrium geometry of the  $X^2A'$  state we find that the  $A^2A''((n_{\text{O}}^-)^{-1})$  state is 0.53 eV higher in energy. Separate calculations on this  $A^2A''((n_{\text{O}}^-)^{-1})$  state at the UB3LYP/6-311+G\* level show that it has a vertical and adiabatic ionization energy of 10.099 and 10.019 eV, respectively. The present calculations thus lead to the conclusion that with respect to maleimide a reversal of the two lower ionic states has taken place in N-methyl maleimide, but also that the two states remain close in energy.

The prediction that the  $(\pi_{\text{N}})^{-1}$  state is the ionic ground state of N-methyl maleimide is at odds with the conclusions

TABLE VIII. Description of the ground and lower-lying electronic singlet states of neutral N-methylmaleimide and of the ground and first excited states of its radical cation. For the neutral molecule excitation energies and oscillator strengths have been calculated by TD-DFT at the B3LYP/6-311+G\* optimized  $S_0$  ( $1^1A'$ ) geometry; for the radical cation excitation energies have been calculated by TD-DFT at the UB3LYP/3-311+G\* optimized geometry of the  $D_0$  ( $X^2A'$ ) state of the radical cation. The excitation energies between parentheses refer to a TD-DFT calculation at the UB3LYP/6-311+G\* optimized  $S_0$  ( $1^1A'$ ) geometry using the orbitals of the  $D_0$  ( $X^2A'$ ) state.

State	Description	Energy (eV)	Oscillator strength
$S_0$ ( $1^1A'$ )	$(\pi_{\text{C=C}})^2(n_{\text{O}}^+)^2(\pi_{\text{N}})^2(n_{\text{O}}^-)^2$	0	
$S_1$ ( $2^1A'$ )	$(\pi_{\text{C=C}})^2(n_{\text{O}}^+)^2(\pi_{\text{N}})^2(n_{\text{O}}^-)^1(\pi_{\text{C=C}}^*)^1$	3.45	0.0000
$S_2$ ( $1^1A''$ )	$(\pi_{\text{C=C}})^2(n_{\text{O}}^+)^2(\pi_{\text{N}})^1(n_{\text{O}}^-)^2(\pi_{\text{C=C}}^*)^1$	3.99	0.0077
$S_3$ ( $2^1A''$ )	$(\pi_{\text{C=C}})^2(n_{\text{O}}^+)^1(\pi_{\text{N}})^2(n_{\text{O}}^-)^2(\pi_{\text{C=C}}^*)^1$	4.17	0.0008
$S_4$ ( $3^1A''$ )	$(\pi_{\text{C=C}})^1(n_{\text{O}}^+)^2(\pi_{\text{N}})^2(n_{\text{O}}^-)^2(\pi_{\text{C=C}}^*)^1$	5.65	0.2813
$D_0$ ( $X^2A'$ )	$(\pi_{\text{C=C}})^2(n_{\text{O}}^+)^2(\pi_{\text{N}})^1(n_{\text{O}}^-)^2$	0 (0.0)	
$D_1$ ( $A^2A''$ )	$(\pi_{\text{C=C}})^2(n_{\text{O}}^+)^2(\pi_{\text{N}})^2(n_{\text{O}}^-)^1$	0.53 (0.0)	
$D_2$ ( $B^2A'$ )	$(\pi_{\text{C=C}})^2(n_{\text{O}}^+)^1(\pi_{\text{N}})^2(n_{\text{O}}^-)^2$	1.55 (0.69)	
$D_3$ ( $C^2A'$ )	$(\pi_{\text{C=C}})^1(n_{\text{O}}^+)^2(\pi_{\text{N}})^2(n_{\text{O}}^-)^2$	1.59 (0.87)	

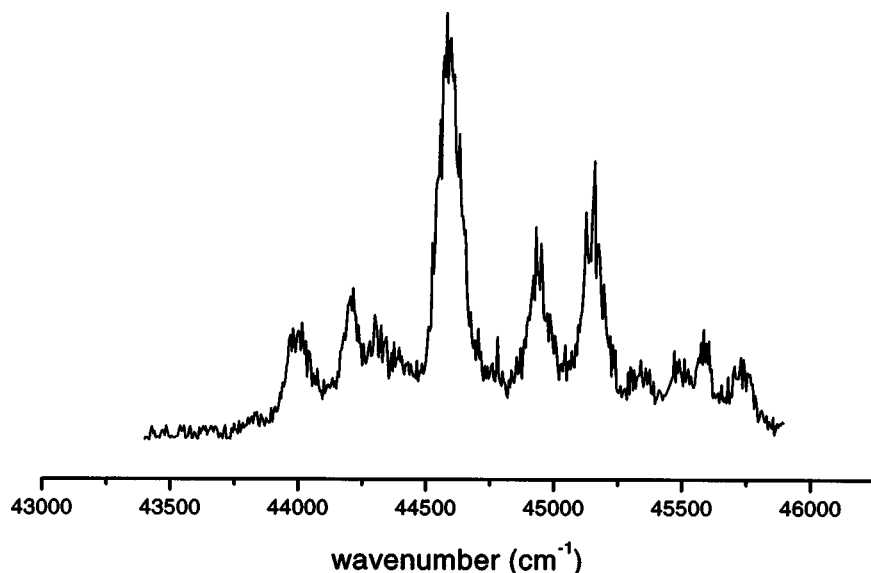


FIG. 5. (1+1) REMPI excitation spectrum of effusively introduced N-methyl maleimide.

reached by Robin<sup>43</sup> In that study it was initially remarked that the large difference between the first ionization potentials of N-methyl maleimide and maleic anhydride might be taken as an indication that ionization occurs from a  $\pi$  orbital rather than a lone pair, but this was later refuted on the basis of lone pair ionizations in simple acids and amides.<sup>47</sup> Although the ordering of the first two electronic ionization limits may therefore still be a matter of debate, this issue is less important for the interpretation of the photoelectron spectra obtained in the present study. It is clear, however, that the elucidation of the electronic structure of the radical cation would greatly benefit from additional He(I) photoionization studies.

In maleimide, considerable mixing occurred between the  $(\pi_N)^{-1}$  and  $(\pi_{C=C})^{-1}$  configurations. In N-methyl maleimide this mixing is nearly absent. At the equilibrium geometry of the  $X^2A'$  state, the  $C^2A'((\pi_{C=C})^{-1})$  state is calculated to have an excitation energy of 1.59 eV, but this is lowered to 0.87 eV at the equilibrium geometry of  $S_0$ . When we now consider the ionization routes of the various excited states in light of these calculations, we have to conclude that in N-methyl maleimide the situation is quite different from that in maleimide. Table VIII shows that in a one-configuration description of excited- and ionic states  $S_4$  ionizes dominantly to  $D_3$ . The calculations predict that this pathway requires more energy than in maleimide, where  $S_4$  could ionize to  $D_1$  as a result of heavy mixing between the  $(\pi_N)^{-1}$  and  $(\pi_{C=C})^{-1}$  configurations. It might well be therefore that ionization to the parent ionic state of  $S_4$  is energetically not possible in one-color REMPI experiments via  $S_4$ . On the other hand, on the basis of symmetry arguments we can also foresee that ionization of  $S_4$  to the  $X^2A'((\pi_N)^{-1})$  state becomes rapidly allowed beyond the one-configuration picture.

## 2. Multiphoton ionization and excited-state photoelectron spectroscopy

N-methyl maleimide has been investigated in the one-photon excitation region of 44 000–45 500  $\text{cm}^{-1}$  under room temperature as well as supersonically cooled conditions. Pre-

vious absorption experiments<sup>24</sup> and our *ab initio* calculations lead us to believe that at these energies excitation of  $S_4$  should take place. Figure 5 shows the (1+1) REMPI excitation spectrum obtained on effusively introduced N-methyl maleimide. The resonances observed in this spectrum are tabulated in Table IX, where the excitation energies reported for the vapor absorption spectrum are also given. Comparison of the two spectra shows that the absorption spectrum is shifted by 35  $\text{cm}^{-1}$  to the blue with respect to the REMPI excitation spectrum. Some further remarks on the assignment of the bands in the spectrum are in order. The availability of the experimental frequencies in the ground state enables us to come to a straightforward assignment of the two strong hot bands, the other (broad) hot band 280  $\text{cm}^{-1}$  below the origin transition probably consists of several transitions and cannot be assigned unambiguously. Previously, the 349  $\text{cm}^{-1}$  band to the blue of the  $0_0^0$  transition was assigned as an overtone of a 182  $\text{cm}^{-1}$  vibration.<sup>24</sup> In our opinion, this cannot be reconciled with the intensity of the higher overtones and with the intensities as measured in the present study. We

TABLE IX. Observed resonances in the (1+1) REMPI excitation spectrum of N-methyl maleimide of  $S_4$  depicted in Fig. 5.

Excitation energy ( $\text{cm}^{-1}$ )	Shift <sup>a</sup>	Assignment	Absorption <sup>b</sup>
43 995	-596	$15_0^0$	44 014
44 204	-387	$16_1^0$	44 228
~44 310	~280		44 346
44 591	0	$0_0^0$	44 623
44 940	349	$16_0^1$	44 984
45 152	561	$15_0^1$	45 188
45 330	739	$13_0^1$	45 372
45 493	902	$16_0^1 15_0^1$	45 537
45 587	996	$11_0^1$ or $10_0^1$	45 620
45 728	1137	$15_0^2$	45 767

<sup>a</sup>Shift with respect to 0-0 transition.

<sup>b</sup>Absorption spectrum of N-methylmaleimide vapor reported by Seliskar and McGlynn (Ref. 24).

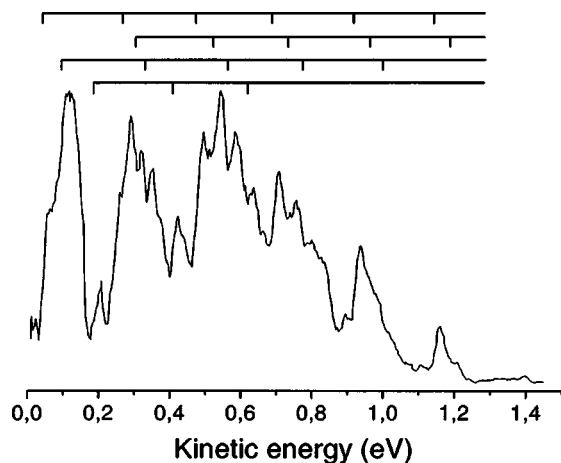


FIG. 6. Excited-state photoelectron spectrum of the vibrationless  $S_4$  excited state of N-methyl maleimide excited at  $44\,590\text{ cm}^{-1}$ .

therefore reassign it to the  $16_0^1$  transition. Similarly, the weak  $739\text{ cm}^{-1}$  band is reassigned to the  $13_0^1$  transition.

In order to get more detailed information on the spectroscopic and dynamic properties of the excited state, an excited-state photoelectron spectrum was measured at the maximum of the origin transition ( $44\,590\text{ cm}^{-1}$ ). This spectrum, shown in Fig. 6, was recorded employing effusively introduced N-methyl maleimide and at a relatively high laser power. Essentially the same spectra could be obtained under supersonically cooled conditions and at a lower laser power, but with a considerably worse signal-to-noise ratio. When trying to assign the photoelectron spectrum, one rapidly comes to the conclusion that the various peaks can be ordered in series involving average steps of  $221\text{ meV}$  ( $1783\text{ cm}^{-1}$ ). This frequency agrees nicely with the frequency calculated for the C=O stretch vibration  $\nu_4^+$  in the ionic ground state. The first series has a clear first member at  $1.160\text{ eV}$  and goes up to five vibrational quanta of  $\nu_4^+$ . A similar series seems to start at  $1.211\text{ eV}$  and can be followed up to  $\nu_4^+ = 4$ . A third series is shifted by  $\sim 130\text{ meV}$  ( $\sim 1100\text{ cm}^{-1}$ ) from the first series, and, on the basis of Table VII, probably involves ionization to combination levels of  $n\nu_4^+$  and  $\nu_8^+ = 1$ . The apparent first member of a last series involving  $\nu_4^+$  is seen at a photoelectron energy of  $0.636\text{ eV}$ . Most probably, there are other members of this series at higher photoelectron energies, but they have too low an intensity, or are overlapped by other stronger bands. It is therefore not known on which mode this series is built.

For an absolute assignment we need to know where the  $0''-0_0^+$  peak is located. One possible choice is to assign the  $1.160\text{ eV}$  peak to the  $0''-0_0^+$  peak and the  $1.211\text{ eV}$  peak to a hot band, i.e., to an ionization process that starts in a vibrationally excited level of the ground state. This assignment implies that the adiabatic ionization energy to  $D_0$  is  $9.897\text{ eV}$ . The intensity distribution in the photoelectron spectrum suggests, however, that the whole assignment might also be shifted by one (or more) quanta of the C=O stretch vibration. The spectrum in Fig. 6 shows indeed a very small peak around  $1.4\text{ eV}$ . If this peak is real—but the present experimental conditions do not allow us to make a decision on

this—then the  $1.160$  and  $1.182\text{ eV}$  peaks can be readily (re)assigned as the  $\nu_5^+ = 1$  and  $\nu_4^+ = 1$  peaks.

For maleimide, the photoelectron spectrum via  $S_4$  showed two ionization routes. The dominant one involved ionization to one particular—in that case excited—ionic state with a propensity for conservation of vibrational energy. In the other one, high-lying vibrational levels of a lower-lying excited state were ionized to the ground ionic state, a process in which dispersal of vibrational energy occurred. The photoelectron spectrum in Fig. 6 is qualitatively different: one would, in fact, be led to conclude that all that is seen here is ionization to the ground ionic state. This might be due to the inaccessibility of the corresponding ionization continua of  $S_4$  as suggested by the calculations, or to a larger dispersal of  $S_4$  character over lower-lying electronic states, which is expected to be enhanced on account of the larger density of states introduced by the methyl substituent. Even without explicit assignment of the various peaks, it is clear that we deal here either with ionization involving very large changes in geometry, or ionization of one or more states with a large vibrational content. Based upon our interpretation of the maleimide spectrum, we conclude that the latter is the case.

The dominant activity of the C=O stretch vibration is another indication that the photoionization process of N-methyl maleimide via  $S_4$  differs more than one would intuitively assume from its parent compound maleimide, where ionization to  $D_0$  was accompanied by activity of the ring deformation mode  $\nu_8$  and the C=C stretch vibration  $\nu_4$ . In principle, two explanations for this difference come to mind. A first explanation is that in maleimide  $S_4$  is coupled to other states than in N-methyl maleimide. For maleimide we reached the conclusion that  $S_3$  is most probably coupled to  $S_4$ ; for N-methyl maleimide we would be talking about a state other than  $S_3$  that undergoes large changes in the carbonyl bonds upon ionization. A second explanation is simply that the ground ionic state of the two molecules is different. Our calculations suggest that the second explanation is the correct one.

#### IV. CONCLUSIONS

We have investigated the spectroscopic and dynamic properties of the strongly one-photon absorbing  $S_4(\pi_{\text{C}=\text{C}}\pi^*)$  state of maleimide and N-methyl maleimide. To this purpose, an experimental approach was combined with *ab initio* calculations of the electronic structure of the molecules. Experimentally, we have found that the wave function of the excited state can be probed in detail by projection on the ionic manifold using excited-state photoelectron spectroscopy. These experiments demonstrate that ionization of maleimide excited to  $S_4$  occurs along several pathways. On the one hand, a channel has been identified that in a one-configuration picture can be described as ionization of the  $\pi^*$  electron from the  $\pi_{\text{C}=\text{C}}\pi^*$  excited state. This channel leads to an electronically excited ionic state with an experimental excitation energy that is in excellent agreement with the *ab initio* predicted one. The experiments show as well that the ionization process populates a broad range of vibrational levels in the ionic ground state, which



can only be explained if we go beyond the one-configuration picture. On the basis of *ab initio* calculated displacement parameters between various excited states and the ionic ground state, it has been argued that the observed Franck–Condon pattern demonstrates that an electronic state is ionized that does not only contain  $S_4$  character but also that of lower-lying states, in particular that of the  $S_3(\pi_N\pi^*)$  state.

Our experiments and calculations demonstrate that N-methyl substitution of the molecule leads to large changes, in particular for the ionic manifold where the ground ionic state is now calculated to be associated with the  $(\pi_N)^{-1}$  configuration as opposed to the  $(n_o^-)^{-1}$  configuration in maleimide. This prediction is in excellent agreement with the dominant activity of the C=O stretch vibration seen in excited-state photoelectron spectra of  $S_4$ . In contrast to maleimide, these spectra do not show clearly multiple ionization pathways, although the observed Franck–Condon pattern strongly suggests a dominant role of internal conversion.

Until the present study, the ionic manifold of the two molecules was virtually unexplored. Apart from elucidating the composition and properties of the  $S_4$  state, the present experiments have also enabled us to obtain information on the spectroscopic properties of this manifold in the form of ionization energies and vibrational frequencies.

## ACKNOWLEDGMENTS

The authors wish to thank Ing. D. Bebelaar for valuable experimental assistance, and Professor C. A. de Lange and Professor M. Glasbeek for use of equipment.

- <sup>1</sup>D. H. A. ter Steege, A. C. Wirtz, and W. J. Buma, *J. Chem. Phys.* **116**, 1 (2002).
- <sup>2</sup>D. H. A. ter Steege, C. Lagrost, and W. J. Buma, *J. Chem. Phys.* **117**, 8270 (2002).
- <sup>3</sup>V. Blanchet, M. Z. Zgierski, and A. Stolow, *J. Chem. Phys.* **114**, 1194 (2001).
- <sup>4</sup>M. Schmitt, S. Lochbrunner, J. P. Shaffer, J. J. Larsen, M. Z. Zgierski, and A. Stolow, *J. Chem. Phys.* **114**, 1206 (2001).
- <sup>5</sup>S.-H. Lee, K.-C. Tang, I.-C. Chen, M. Schmitt, J. P. Schaffer, T. Schultz, J. G. Underwood, M. Z. Zgierski, and A. Stolow, *J. Phys. Chem. A* **106**, 8979 (2002).
- <sup>6</sup>R. A. Rijkenberg, W. J. Buma, C. A. van Walree, and L. W. Jenneskens, *J. Phys. Chem. A* **106**, 5249 (2002).
- <sup>7</sup>C. E. Hoyle, K. Viswanathan, S. C. Clark, C. W. Miller, C. Nguyen, S. Jönsson, and L. Shao, *Macromolecules* **32**, 2793 (1999).
- <sup>8</sup>M. Shimose, C. E. Hoyle, S. Jönssen, P. E. Sundell, J. Owens, and K. Vaughn, *Polym. Prepr. (Am. Chem. Soc. Div. Polym. Chem.)* **36**, 485 (1995).
- <sup>9</sup>S. Jönsson, P. E. Sundell, J. Hultgren, D. Sheng, and C. E. Hoyle, *Prog. Org. Coat.* **27**, 107 (1996).
- <sup>10</sup>C. Decker, F. Morel, S. C. Clark, S. Jönssen, and C. E. Hoyle, *Polym. Mater. Sci. Eng.* **75**, 198 (1996).
- <sup>11</sup>H. Andersson, U. W. Gedde, and A. Hult, *Macromolecules* **29**, 1649 (1996).
- <sup>12</sup>H. Andersson, U. W. Gedde, and A. Hult, *J. Coat. Technol.* **69**, 91 (1997).
- <sup>13</sup>C. E. Hoyle, S. C. Clark, S. Jönssen, and M. Shimose, *Polymer* **38**, 5695 (1997).
- <sup>14</sup>S. Jönssen, P. E. Sundell, M. Shimose, S. C. Clark, C. Miller, F. Morel, C. Decker, and C. E. Hoyle, *Nucl. Instrum. Methods Phys. Res. B* **131**, 276 (1997).
- <sup>15</sup>P. Kohli, A. B. Scranton, and G. J. Blanchard, *Macromolecules* **31**, 5681 (1998).
- <sup>16</sup>C. E. Hoyle, S. C. Clark, S. Jönssen, and M. Shimose, *Polym. Commun.* **38**, 5695 (1998).
- <sup>17</sup>C. W. Miller, S. Jönssen, C. E. Hoyle, C. Hasselgren, T. Haraldson, and L. Shao, *RadTech'98 Proc.* 182 (1998).
- <sup>18</sup>J. von Sonntag and W. Knolle, *J. Photochem. Photobiol., A* **136**, 133 (2000).
- <sup>19</sup>S. C. Clark, Ph.D. dissertation, Department of Polymer Science, The University of Southern Mississippi, Hattiesburg, MS, 1999.
- <sup>20</sup>J. von Sonntag, Ph.D. dissertation, Faculty of Chemistry and Mineralogy, The University of Leipzig, Germany, 1999.
- <sup>21</sup>J. M. Warman, R. D. Abellon, H. J. Verhey, J. W. Verhoeven, and J. W. Hofstraat, *J. Phys. Chem. B* **101**, 4913 (1997).
- <sup>22</sup>B. Kükrer Kaletas, R. M. Williams, B. König, and L. De Cola, *Chem. Commun. (Cambridge)* **2002**, 776.
- <sup>23</sup>T. Matsuo, *Bull. Chem. Soc. Jpn.* **38**, 557 (1965).
- <sup>24</sup>C. J. Seliskar and S. P. McGlynn, *J. Phys. Chem.* **55**, 4337 (1971).
- <sup>25</sup>C. J. Seliskar and S. P. McGlynn, *J. Phys. Chem.* **56**, 275 (1972).
- <sup>26</sup>C. J. Seliskar and S. P. McGlynn, *J. Phys. Chem.* **56**, 1471 (1972).
- <sup>27</sup>C. R. Scheper, W. J. Buma, and C. A. de Lange, *J. Electron Spectrosc. Relat. Phenom.* **109**, 8319 (1998).
- <sup>28</sup>A. M. Rijs, E. H. G. Backus, C. A. de Lange, N. P. C. Westwood, and M. H. M. Janssen, *J. Electron Spectrosc. Relat. Phenom.* **112**, 151 (2000).
- <sup>29</sup>P. Kruit and F. H. Read, *J. Phys. E* **16**, 313 (1983).
- <sup>30</sup>C. E. Moore, *Atomic Energy Levels*, Natl. Bur. Stand. (U.S.) Circ. No. 35 (U.S. GPO, Washington, DC, 1971), Vol. II.
- <sup>31</sup>M. J. Frisch, G. W. Trucks, H. B. Schlegel *et al.*, GAUSSIAN 98, Revision A.5; Gaussian, Inc., Pittsburgh, PA, 1998.
- <sup>32</sup>M. W. Schmidt, K. K. Baldrige, J. A. Boatz *et al.*, *J. Comput. Chem.* **14**, 1347 (1993).
- <sup>33</sup>W. J. Buma and F. Zerbetto, *J. Chem. Phys.* **103**, 10492 (1995).
- <sup>34</sup>E. V. Doktorov, I. A. Malkin, and V. I. Man'ko, *J. Mol. Spectrosc.* **64**, 302 (1977).
- <sup>35</sup>R. A. Rijkenberg and W. J. Buma, *J. Phys. Chem. A* **106**, 3727 (2002).
- <sup>36</sup>M. J. Frisch, J. A. Pople, and J. S. Binkley, *J. Chem. Phys.* **80**, 3265 (1984).
- <sup>37</sup>J. B. Foresman, M. Head-Gordon, J. A. Pople, and M. J. Frisch, *J. Phys. Chem.* **96**, 135 (1992).
- <sup>38</sup>A. M. Becke, *J. Chem. Phys.* **98**, 5648 (1993).
- <sup>39</sup>L. Harsanyi, E. Vajda, and I. Hargittai, *J. Mol. Struct.* **129**, 315 (1985).
- <sup>40</sup>T. Wolbaek, P. Klaboe, and C. J. Nielsen, *J. Mol. Struct.* **27**, 283 (1975).
- <sup>41</sup>T. Wolbaek, P. Klaboe, and C. J. Nielsen, *J. Mol. Struct.* **28**, 269 (1975).
- <sup>42</sup>A. J. Barnes, L. Le Gall, C. Madec, and J. Lauransan, *J. Mol. Struct.* **38**, 109 (1977).
- <sup>43</sup>M. B. Robin, *Higher Excited States of Polyatomic Molecules* (Academic, New York, 1975), Vol. II.
- <sup>44</sup>P. M. Weber and N. Thant, *Chem. Phys. Lett.* **197**, 556 (1992).
- <sup>45</sup>B. Kim, C. P. Schick, and P. M. Weber, *J. Chem. Phys.* **103**, 6903 (1995).
- <sup>46</sup>S. Hillenbrand, L. Zhu, and P. Johnson, *J. Chem. Phys.* **92**, 870 (1990).
- <sup>47</sup>C. R. Brundle, D. W. Turner, M. B. Robin, and H. Basch, *Chem. Phys. Lett.* **3**, 292 (1969).
- <sup>48</sup>P. J. Cox and S. F. Parker, *Acta Crystallogr., Sect. C: Cryst. Struct. Commun.* **52**, 2578 (1996).
- <sup>49</sup>A. P. Scott and L. Radon, *J. Phys. Chem.* **100**, 16502 (1996).
- <sup>50</sup>S. F. Parker, *Spectrochim. Acta, Part A* **51**, 2067 (1995).